

- Smith, W. W., Pattridge, K. A., & Ludwig, M. L. (1983) *J. Mol. Biol.* 165, 737–755.
- Staden, R. (1982a) *Nucleic Acids Res.* 10, 4731–4751.
- Staden, R. (1982b) *Nucleic Acids Res.* 10, 2951–2961.
- Staden, R. (1985) in *Genetic Engineering: Principles and Methods* (Setlow, J. K., & Hollaender, A., Eds.) pp 67–114, Plenum Publishing Corp., New York and London.
- Suggs, S. V., Hirose, T., Miyake, T., Kawashima, E. H., Johnson, M. J., Itakura, K., & Wallace, R. B. (1981) in *Developmental Biology Using Purified Genes* (Brown, D. D., Ed.) pp 683–693, Academic Press, New York and London.
- Taylor, S. S. (1977) *J. Biol. Chem.* 252, 1799–1806.
- Tran-Betcke, A., Warnecke, U., Böcker, C., Zabarosch, C., & Friedrich, B. (1990) *J. Bacteriol.* 172, 2920–2929.
- van Belzen, R., & Albracht, S. P. J. (1989) *Biochim. Biophys. Acta* 974, 311–320.
- Viñas, O., Powell, S. J., Runswick, M. J., Iacobazzi, V., & Walker, J. E. (1990) *Biochem. J.* 265, 321–326.
- Vogelstein, B., & Gillespie, D. (1979) *Proc. Natl. Acad. Sci. U.S.A.* 76, 615–619.
- Volokita, M., & Somerville, C. R. (1987) *J. Biol. Chem.* 262, 15825–15828.
- von Heijne, G. (1986) *EMBO J.* 5, 1335–1342.
- Walker, J. E., Powell, S. J., Viñas, O., & Runswick, M. J. (1989) *Biochemistry* 28, 4702–4708.
- Weijer, W. J., Hofsteenge, J., Vereijken, J. M., Jekel, P. A., & Beintema, J. J. (1982) *Biochim. Biophys. Acta* 704, 385–388.
- White, J. L., Hackert, M. L., Buehner, M., Adams, M. J., Ford, G. C., Lentz, P. J., Jr., Smiley, I. E., Steindel, S. J., & Rossmann, M. G. (1978) *J. Mol. Biol.* 102, 759–779.
- Wierenga, R. K., & Hol, W. G. (1983) *Nature* 302, 842–844.
- Wierenga, R. K., De Jong, R. J., Kalk, K. H., Hol, W. G. J., & Drenth, J. (1979) *J. Mol. Biol.* 131, 55–73.
- Wierenga, R. K., Terpstra, P., & Hol, W. G. J. (1986) *J. Mol. Biol.* 187, 101–107.
- Wikström, M. (1984) *FEBS Lett.* 169, 300–304.
- Xia, Z.-X., Shamala, N., Bethge, P. H., Lim, L. W., Bellamy, H. D., Xuong, N. H., Lederer, F., & Mathews, F. S. (1987) *Proc. Natl. Acad. Sci. U.S.A.* 84, 2629–2633.
- Yasunobu, K., & Tanaka, M. (1980) *Methods Enzymol.* 69, 228–238.
- Young, I. G., Rogers, B. L., Campbell, H. D., Jaworowski, A., & Shaw, D. C. (1981) *Eur. J. Biochem.* 116, 165–170.

Structural Study of Porcine Pancreatic Elastase Complexed with 7-Amino-3-(2-bromoethoxy)-4-chloroisocoumarin as a Nonreactivable Doubly Covalent Enzyme–Inhibitor Complex^{†,‡}

J. Vijayalakshmi,[§] Edgar F. Meyer, Jr.,^{*§} Chih-Min Kam,^{||} and James C. Powers^{||}

Department of Biochemistry and Biophysics, Texas A&M University, College Station, Texas 77843-2128, and School of Chemistry, Georgia Institute of Technology, Atlanta, Georgia 30332-0400

Received August 6, 1990; Revised Manuscript Received October 17, 1990

ABSTRACT: The complex of porcine pancreatic elastase (PPE) with 7-amino-3-(2-bromoethoxy)-4-chloroisocoumarin, a potent mechanism-based inhibitor, was crystallized and the crystal structure determined at 1.9-Å resolution with a final *R* factor of 17.1%. The unbiased difference Fourier electron density map showed continuous density from O γ of Ser 195 to the benzoyl carbonyl carbon atom and from N ϵ 2 of His 57 to the carbon atom at the 4-position of the isocoumarin ring in the inhibitor. This suggested unambiguously that the inhibitor was doubly covalently bound to the enzyme. It represents the first structural evidence for irreversible binding of an isocoumarin inhibitor to PPE through both Ser 195 and His 57 in the active site. The PPE–inhibitor complex is only partially activated in solution by hydroxylamine and confirms the existence of the doubly covalently bound complex along with the acyl enzyme. The benzoyl carbonyl oxygen atom of the inhibitor is not situated in the oxyanion hole formed by the amide (>NH) groups of Gly 193 and Ser 195. The complex is stabilized by the hydrogen-bonding interactions in the active site (from the N ϵ 2 of Gln 192 to the bromine atom in the inhibitor and the amino group at the 7-position of the isocoumarin ring to the carbonyl oxygen of Thr 41) and by van der Waals interactions. The inhibition rates of several 7-substituted 4-chloro-3-(bromoalkoxy)isocoumarins toward PPE were measured. The *N*-alkylureido and *N*-(arylalkyl)ureido derivatives are more potent inhibitors of PPE than 7-amino-3-(2-bromoethoxy)-4-chloroisocoumarin due to a proposed favorable interaction between the *N*-alkyl group of the inhibitors and the hydrophobic subsites S $_2$ ' or S $_3$ ' subsites.

Serine proteases are capable of cleaving connective tissue proteins such as elastin as well as destroying invading bacteria.

[†]This work was supported by grants from the Robert A. Welch Foundation and the Texas Agricultural Experiment Station to E.F.M. and from the National Institutes of Health to J.C.P. (HL 29307).

[‡]Coordinates of the title complex are being submitted to the Brookhaven Protein Data Bank and are designated as 9EST.

^{*}To whom correspondence should be addressed.

[§]Texas A&M University.

^{||}Georgia Institute of Technology.

Excessively high levels of these proteases in the system or a functional deficiency of natural inhibitors to these proteases, such as α 1-protease inhibitor, can cause inflammatory diseases such as pulmonary emphysema (Lungarella et al., 1985; Powers, 1976), arthritis (Janoff, 1973, 1978), pancreatitis (Geokas et al., 1968), adult respiratory distress syndrome (Burchardi et al., 1984), and certain degenerative skin disorders. The importance of serine proteases as pathogenic agents in a variety of diseases has stimulated considerable

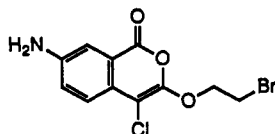


FIGURE 1: Structure of 7-amino-3-(2-bromoethoxy)-4-chloroisocoumarin.

interest in the design of mechanism-based, non-peptidyl, heterocyclic inhibitors for these enzymes. A variety of heterocyclic mechanism-based inhibitors including isocoumarins has recently been investigated and shown to be effective inactivators of several serine proteases and thus potential drugs for the treatment of a variety of diseases (Powers & Harper, 1986).

Kinetic and crystallographic studies have shown that these mechanism-based inhibitors initially react with Ser 195 in the active site to produce an acyl enzyme, unmasking in the process another functional group which subsequently reacts with other active site residues such as His 57. Kinetic studies (Harper & Powers, 1985) have shown that isocoumarins substituted with 7-amino and 4-chloro groups react with serine protease to form very stable derivatives. In the reaction of these inhibitors, the unmasked functional group is a postulated quinone imine methide intermediate which invites nucleophilic attack by His 57 and results in complete inactivation through the formation of a second covalent bond to the enzyme.

Isocoumarins with 3-methoxy, 3-ethoxy, or 3-(2-bromoethoxy) substituents are the most effective elastase inhibitors among the 3-alkoxy-7-amino-4-chloroisocoumarins studied (Powers et al., 1990). This observation has been confirmed by the present crystal structure analysis of the 7-amino-3-(2-bromoethoxy)-4-chloroisocoumarin (Figure 1) complex with PPE. The crystallographic data of the complex were measured to 1.9-Å resolution. The initial unbiased electron density difference map showed continuous density, indicative of covalent linkages of the inhibitor with the active site Ser 195 and His 57 residues.

The previous analyses of PPE¹ complexes with 7-amino-4-chloro-3-methoxyisocoumarin (Meyer et al., 1985) and 4-chloro-3-ethoxy-7-guanidinoisocoumarin (Powers et al., 1990) have resulted only in acyl enzyme complexes. The different binding modes of these two earlier isocoumarin complexes with PPE and the present one are summarized in this report. Subsequent to this structure analysis, we have also observed that 4-chloro-3-ethoxy-7-guanidinoisocoumarin, a potent thrombin inhibitor, is also doubly covalently bound to bovine trypsin and form an acylated enzyme (Chow et al., 1990). Markedly different modes of binding were observed in these two doubly covalently bound complexes of isocoumarins with trypsin and elastase. The present study is a further illustration of the variety of binding modes that are observed in complexes of heterocyclic inhibitors with serine proteases.

EXPERIMENTAL PROCEDURES

A solution of PPE and the 7-amino-3-(2-bromoethoxy)-4-chloroisocoumarin was allowed to react in 0.1 M sodium phosphate buffer at pH 5.0 with 7% acetonitrile. The ratio of inhibitor to enzyme was 7:1, and the concentration of the enzyme was 1.2% (w/v). After 7 days crystals of the inhibited enzyme were obtained by vapor diffusion from 0.1 M sodium phosphate and 0.1 M sodium sulfate solution. A crystal of

Table I: Crystallographic Parameters and Final Refinement Statistics for the Structure of the Complex of PPE with 7-Amino-3-(2-bromoethoxy)-4-chloroisocoumarin

crystal size	0.5 × 0.4 × 1.0 mm ³
cell dimensions (Å)	a = 51.13, b = 58.14, c = 75.45
data collection temperature (°C)	19
resolution range of data (Å)	6.0–1.9
space group	P212121
effective resolution (Å) (Swanson, 1988)	2.05
no. of atoms/asymmetric unit	1977
no. of unique reflections above 2σ level	11 586
completeness of data	65%
$\langle 1/\sigma \rangle$	8.81
R factor ($R = \sum F_o - F_c / \sum F_o $)	0.171
overall temperature factor of 1961 atoms in protein weighted as per electron count (Å ²)	24.2
overall temperature factor of the inhibitor atoms (Å ²)	40.2
σ of 1888 bond lengths (Å)	0.010
σ of 2577 bond angles (deg)	1.2
features of final residual difference density map (e/Å ³)	
min height (Å)	-0.48
max height (Å)	0.37
σ (Å)	0.08
mean positional error (Å) (Luzzati, 1952)	0.2

dimensions 0.5, 0.4, and 1.0 mm was chosen for data collection. The crystal was mounted in a capillary in contact with traces of buffer and a small quantity of fresh, solid inhibitor. Diffraction data were collected in 10 days by using the rotation method with a flat plate precession camera modified for oscillation photography (Huber-Rimsting Model 206). For data collection, a 21-year-old Nonius generator operating at 35 kV and 32 mA and a Seifert Cu anode sealed X-ray tube were used to produce Ni-filtered radiation; a 0.3-mm collimator was used. Data collection was carried out with a crystal rotation rate of 3°/600 min over the rotation range of 102° on the spindle axis, with a crystal to film distance of 52 mm, and with the crystal c axis approximately along the rotation axis. The crystal was deliberately misaligned by 11.7° and -18.9° with respect to the y and z camera axes, permitting the use of an accelerated data collection procedure (Radhakrishnan et al., 1987). After the collection to 78° had been completed, the crystal was found to have shifted from its original position. The new missetting angles of 5.0° and -1.0° were used for the remainder of the measurements.

The reflection intensities were measured by using an Optonics P-1000 microdensitometer. The intensities were evaluated by using the program FILME (Schwager & Bartels, 1975) to evaluate screenless precession or rotation films from protein crystals. Data to 1.9-Å resolution contained 11 586 unique reflections above the 2σ level and were 65% complete for a total of 17 673 possible reflections; the last shell (1.94–1.9-Å resolution) was 35% complete. The agreement of equivalent reflections within each film varied from 2.9% to 10.3% (R_{sym} values) whereas the agreement in the measurement of equivalent reflections with their mean values from different films (R_{merge} values) varied from 8.2% to 12.3%. The final film pack showed that the crystal had begun to crack. This set of films had high values for R_{sym} (11.8%) and R_{merge} (15.1%) values and was subsequently rejected. The crystal cell dimensions and the missetting angles were refined by using the program MADNES (Messerschmidt & Pflugrath, 1987). The crystal data are given in Table I. Due to the unavoidable use of a superannuated generator and hence weak X-ray source, the data and various estimates of agreement are not commensurate with our usual standards; nevertheless, the data are quite adequate for the subsequent structure analysis.

¹ Abbreviations: TNT, Ten Eyck–Tronrud refinement package; PPE, porcine pancreatic elastase; HLE, human leukocyte elastase; rms, root mean square.

Table II: List of Crystallographic Studies of Heterocyclic Inhibitor Complexes with Porcine Pancreatic Elastase

inhibitor compound	R factor (%)	resolution (Å)	no. of reflections
β -lactam inhibitor (Navia et al., 1987)	22.8	1.84	14 135
two valine-derived benzoxazinones (Radhakrishnan et al., 1987)	17.2	1.76	16 320
7-amino-4-chloro-3-methoxyisocoumarin (Meyer et al., 1988)	18.0	1.80	15 614
4-chloro-3-ethoxy-7-guanidinoisocoumarin (Powers et al., 1990)	17.0	1.74	16 405
title complex	17.1	1.9	11 586

Crystallographic Modeling and Refinement. The isomorphous native structure (Meyer et al., 1988) including bound water molecules, calcium, and sulfate ions, but omitting the active site sulfate ion and water molecules, was used for initial phasing of the reflections and calculation of a difference Fourier map to locate the inhibitor in the active site. Program TNT, a least-squares refinement program for macromolecular structures (Tronrud et al., 1987), was used for the calculation of maps and refinements. In order to account for small changes in cell dimensions between native and inhibited enzymes, two cycles of positional parameter refinements and one cycle of temperature factor refinement were calculated for the unbiased model ($R = 23\%$) before obtaining the initial difference Fourier map.

A model of the inhibitor was fitted into the electron density map using the Evans & Sutherland PS-330 graphics terminal and program FRODO (Jones, 1978). The model of the molecular complex was constructed in such a way as to be consistent with both the known reaction chemistry of isocoumarins as well as the electron density from the unbiased Fourier maps. It was immediately noticed in the unbiased difference Fourier map that the His 57 side chain was located in the "in" position as in the native structure (Meyer et al., 1988). It should be noted here that the imidazole ring was forced into the "out" position in all previous structures of PPE complexed with heterocyclic inhibitors (Table II). The location of the residual density for His 57, as well as its continuous contact with the density representing the isocoumarin inhibitor, indicated covalent attachment between His 57 and the inhibitor. Ser 195 O γ was in an envelope of electron density continuous with the inhibitor and was likewise covalently attached. Two models, one having the *R* configuration and another having the *S* configuration at the isocoumarin C4 atom bonded to His 57, were generated and compared. The model with the *S* configuration at C4 fit the density better and was therefore used for subsequent refinement.

After fitting the model into density, the positions of the Ca²⁺ and the SO₄²⁻ ions were checked in difference Fourier maps and were found to be conserved relative to the native structure. Most of the water molecules were also found to be close to their corresponding positions in the native structure (Meyer et al., 1988). All were included with the native enzyme coordinates, and the refinement was started with an initial temperature factor of 20 Å² for all non-hydrogen inhibitor atoms.

A regimen of three cycles of atomic positional parameter refinement followed by one cycle of atomic thermal (*B*) factor refinement was generally followed. Geometric constraints were introduced during positional parameter refinements. The *R* factor module (X-ray module) and geometry module were combined with a weighting for the *R* factor of 0.001, for bonds as 1.0, and for angles as 3.0. The TNT default values of weights for torsion, plane, and contact distance were employed. As the form factor for bromine was missing from the TNT library,

Table III: Optimum and Refined Values for the Geometrical Parameters at the Two Covalent Regions between the Inhibitor and the Active Site Ser 195 and His 57 Residues^a

geometric parameters	optimum	refined
C1–O γ	1.35	1.32
C1–O1	1.246	1.21
C1–O γ –C β	117	114.4
C9–C1–O γ	116.0	120.3
O1–C1–O γ	123.0	119.5
C4–N ϵ 2	1.45	1.47
C10–C4–N ϵ 2	109.0	112.1
C3–C4–N ϵ 2	109.0	109.7
C4–N ϵ 2–C ϵ 1	125.0	125.3
C4–N ϵ 2–C δ 2	125.0	126.0

^a Bond lengths in Å and angles in deg.

it was introduced from Lee and Pakes (1969) and the TNT Generalsf program was recompiled and used for F_c calculations. Geometric restraints used for the inhibitor complex at the two covalent sites are given in Table III. The parameters for the covalent bond from N ϵ 2 of His 57 to C4 atom of the inhibitor were taken from volume A1 of *Molecular Structures and Dimensions* (Kennard et al., 1972). The geometric parameters for the ester bond between O γ of active site serine and the benzoyl carbonyl carbon atom of the inhibitor were taken from Schweizer and Dunitz (1982). The Ser 195–inhibitor ester bond and the bond from N ϵ 2 of His 57 to the C4 atom of the inhibitor were treated analogously to a disulfide linkage.

During refinements additional water molecules were revealed in the difference Fourier maps and were identified by the program TNTMAX (S. Swanson, unpublished results) and checked for proper geometry by the program WATER (R. Radhakrishnan, unpublished results). In total, 133 water molecules were located and introduced in two stages. After 630 cycles of refinement, the final *R* factor ($R = \sum ||F_o| - |F_c|| / \sum |F_o|$) was 0.171. The final standard deviations were 0.010 Å for 1888 bond lengths and 1.12° for 2577 bond angles in the sample. The refinement results are given in Table I. The refined parameters specific for the geometry at the two covalent regions of the enzyme inhibitor complex are given in Table III. The overall temperature factor weighed as per electron count was 40.2 Å² for 16 inhibitor atoms and 24.2 Å² for 1961 atoms in the protein. The overall *B* values for Ser 195 and His 57 were 22.1 Å² and 22.9 Å², respectively. The thermal factor for bromine was 50 Å², which is the upper limit for *B* factors specified in the refinement program. Although a heavy atom (Br) is at the end of the bromoethoxy chain, it is not tightly held by the extended binding site of PPE and thus is relatively free to flex with time, which possibly explains the high thermal factor. It is also chemically possible that the terminal Br atom on the bromoethoxy chain could hydrolyze to a hydroxyl group (with release of HBr). Therefore, a structure of 3-(hydroxyethoxy) (OCH₂CH₂OH) was also refined. The hydroxyl O atom refined to a reasonable *B* factor (18 Å²) but at a position too far (3.28 Å) to make reasonable hydrogen bonds with nearby donors and acceptors. The *B* factor of this O atom at the farthest end of the side chain was even less than the next carbon atom (C₁₂) in the chain, probably because it was modeled to fit in a region of electron density which otherwise would have been occupied by a much heavier Br atom. Therefore, in the absence of clear chemical evidence to the contrary, the Br atom was retained and is reported in the final structure.

Materials. Porcine pancreatic elastase was obtained from Sigma Chemical Co., St. Louis, MO. Hepes was purchased from Research Organics Inc., Cleveland, OH, and Suc-Ala-

Ala-Ala-NA was purchased from Peninsula Laboratories, Inc., Belmont, CA. 2-Bromoethanol, 3-bromopropanol, phosphorus pentachloride, phenylacetyl chloride, phenyl isocyanate, and various alkyl isocyanates were obtained from Aldrich Chemical Co., Milwaukee, WI.

Synthesis. Each new compound was checked by NMR, melting point, mass spectroscopy, thin-layer chromatography, and elementary analysis. The results are consistent with the proposed structures. ¹H NMR spectra were recorded on a Varian Model T-60A NMR spectrometer (60 MHz). Mass spectra (MS) were obtained on a Varian MAT Model 112S mass spectrometer. Microanalyses were performed by Atlanta Microlab, Inc. Atlanta, GA. Thin-layer chromatography (TLC) was performed on silica gel glass plates coated with 254-nm fluorescent indicator. TLC for all compounds was developed with a CHCl₃/MeOH = 9:1 solvent system. 7-Amino-3-(2-bromoethoxy)-4-chloroisocoumarin and 7-amino-3-(3-bromopropoxy)-4-chloroisocoumarin were synthesized by a previously described method (Powers et al., 1990). For synthesis of derivatives of 7-amino-3-(bromoalkoxy)-4-chloroisocoumarins, two methods were used.

Method A. Equimolar amounts of 7-amino-3-(bromoalkoxy)-4-chloroisocoumarin and the corresponding isocyanate were mixed in a small amount of dry THF and stirred at room temperature for a few days. During this time yellow crystals slowly formed. After filtration, the compounds were recrystallized once more from THF-pentane.

Method B. An equimolar mixture of 7-amino-3-(bromoalkoxy)-4-chloroisocoumarin, an acyl chloride, and triethylamine in dry THF was stirred overnight. The solution was washed with water, 4% NaHCO₃, and water and dried over MgSO₄. After filtration and evaporation, a yellow residue was crystallized from THF-pentane.

3-(2-Bromoethoxy)-7-[(*tert*-butylcarbamoyl)amino]-4-chloroisocoumarin. This compound was synthesized by method A: yield 45%; mp 165–166 °C; TLC *R_f* = 0.55; MS *m/e* 418 (M⁺ + 1). Anal. Calcd for C₁₈H₁₈N₂O₄ClBr: C, 46.01; H, 4.34. Found: C, 46.05; H, 4.38.

3-(2-Bromoethoxy)-4-chloro-7-[(*isopropyl*carbamoyl)amino]isocoumarin. This compound was synthesized by method A: yield 47%; mp 205–206 °C; TLC *R_f* = 0.58; MS *m/e* 404 (M⁺ + 1). Anal. Calcd for C₁₅H₁₆N₂O₄ClBr: C, 44.63; H, 4.00. Found: C, 44.51; H, 3.97.

3-(2-Bromoethoxy)-4-chloro-7-[(*phenyl*carbamoyl)amino]isocoumarin. This compound was synthesized by method A: yield 41%; mp 215–217 °C; TLC *R_f* = 0.68; MS *m/e* 437 (M⁺ + 1). Anal. Calcd for C₁₈H₁₄N₂O₄ClBr: C, 49.40; H, 3.22; N, 6.40; Cl, 8.10. Found: C, 49.48; H, 3.25; N, 6.34; Cl, 8.12.

7-[(*Benzyl*carbamoyl)amino]-3-(2-bromoethoxy)-4-chloroisocoumarin. This compound was synthesized by method A: yield 44%; mp 200–203 °C; TLC *R_f* = 0.65; MS *m/e* 452 (M⁺ + 1). Anal. Calcd for C₁₉H₁₆N₂O₄ClBr: C, 50.52; H, 3.57. Found: C, 50.59; H, 3.59.

3-(2-Bromoethoxy)-4-chloro-7-[[(*R*)-methylbenzyl]carbamoyl]amino]isocoumarin. This compound was synthesized by method A: yield 66%; mp 183–185 °C; TLC *R_f* = 0.60; MS *m/e* 464 (M⁺). Anal. Calcd for C₂₀H₁₈N₂O₄ClBr: C, 51.58; H, 3.90. Found: C, 51.66; H, 3.90.

3-(2-Bromoethoxy)-4-chloro-7-[[(*S*)-methylbenzyl]carbamoyl]amino]isocoumarin. This compound was synthesized by method A: yield 59%; mp 186–188 °C; TLC *R_f* = 0.60; MS *m/e* 345 (M⁺ - [Ph(CH₃)CHNH] + 1). Anal. Calcd for C₂₀H₁₈N₂O₄ClBr: C, 51.58; H, 3.90. Found: C, 51.60; H, 3.90.

Table IV: Inhibition Rates of PPE by 7-Substituted 3-(Bromoalkoxy)-4-chloroisocoumarins^a

inhibitors	[I] (μM)	<i>k</i> _{obs} /[I] (M ⁻¹ s ⁻¹)
7-substituted		
3-(2-bromoethoxy)-4-chloroisocoumarin		
7-NH ₂	8.3	1000
7-(<i>t</i> -Bu-NHCONH)	8.3	6600
7-(<i>isopropyl</i> -NHCONH)	8.3	4500
7-(PhNHCONH)	42	36
7-(PhCH ₂ NHCONH)	8.3	3000
7-[(<i>R</i>)-(C ₆ H ₅)(CH ₃)CHNHCONH]	8.3	9900
7-[(<i>S</i>)-(C ₆ H ₅)(CH ₃)CHNHCONH]	8.3	2700
7-(PhCH ₂ CONH)	8.3	5000
7-substituted		
3-(2-bromopropoxy)-4-chloroisocoumarin		
7-NH ₂	42	10
7-(PhNHCONH)	83	4
7-(PhCH ₂ NHCONH)	42	13
7-(PhCH ₂ CONH)	40	28

^a Inhibition rates were measured in 0.1 M HEPES, 0.5 M NaCl, pH 7.5 buffer, and 8–9% Me₂SO at 25 °C. The substrate was Suc-Ala-Ala-NA (0.48 mM).

3-(2-Bromoethoxy)-4-chloro-7-[(*phenyl*acetyl)amino]isocoumarin. This compound was synthesized by method B: yield 72%; mp 165–169 °C; TLC *R_f* = 0.65; MS *m/e* 436 (M⁺ + 1). Anal. Calcd for C₁₉H₁₅N₁O₄ClBr: C, 52.26; H, 3.46. Found: C, 52.47; H, 3.71.

3-(3-Bromopropoxy)-4-chloro-7-[(*phenyl*carbamoyl)amino]isocoumarin. This compound was synthesized by method A: yield 38%; mp 192–193 °C; TLC *R_f* = 0.68; MS *m/e* 452 (M⁺ + 1). Anal. Calcd for C₁₉H₁₆N₂O₄ClBr: C, 50.52; H, 3.57. Found: C, 50.62; H, 3.61.

7-[(*Benzyl*carbamoyl)amino]-3-(3-bromopropoxy)-4-chloroisocoumarin. This compound was synthesized by method A: yield 38%; mp 188–189 °C; TLC *R_f* = 0.66; MS *m/e* 466 (M⁺ + 1). Anal. Calcd for C₂₀H₁₈N₂O₄ClBr: C, 51.58; H, 3.90. Found: C, 51.57; H, 3.92.

3-(3-Bromopropoxy)-4-chloro-7-[(*phenyl*acetyl)amino]isocoumarin. This compound was synthesized by method B: yield 74%; mp 151–153 °C; TLC *R_f* = 0.92; MS *m/e* 451 (M⁺ + 1). Anal. Calcd for C₂₀H₁₇NO₄ClBr: C, 53.30; H, 3.80. Found: C, 53.59; H, 4.02.

Inhibition Kinetics. Incubation Method. Inactivation was initiated by adding a 50-μL aliquot of inhibitor in Me₂SO to 0.55 μL of enzyme-buffered solution (1.7 μM) such that final Me₂SO concentration was 8.3% v/v at 25 °C. Aliquots were removed at different time intervals and diluted into substrate solution (240-fold dilution). The residual enzyme activity was measured spectrophotometrically in 0.1 M HEPES and 0.5 M NaCl, pH 7.5, with Suc-Ala-Ala-NA (0.48 mM) as substrate (Nakajima et al., 1979). Peptide *p*-nitroanilide hydrolyses were monitoring at 410 nm (Erlanger et al., 1961). First-order inactivation rate constants (*k*_{obs}) were obtained from plots of ln (*v_t/v₀*) vs time. Inhibitor concentrations are shown in Table IV, and inactivation rate constants were typically the average of the duplicate or triplicate experiments.

RESULTS

X-ray Crystallography. X-ray structure analysis has unambiguously shown that the heterocyclic compound 7-amino-3-(2-bromoethoxy)-4-chloroisocoumarin has formed a double covalent link with the enzyme, which is postulated to begin with initial acylation by Ser 195 followed by nucleophilic attack by His 57. The electron density map (Figure 2) shows continuous density corresponding to the ester covalent linkage formed between Ser 195 O_γ and the benzoyl carbonyl carbon atom of the inhibitor and also corresponding to the covalent

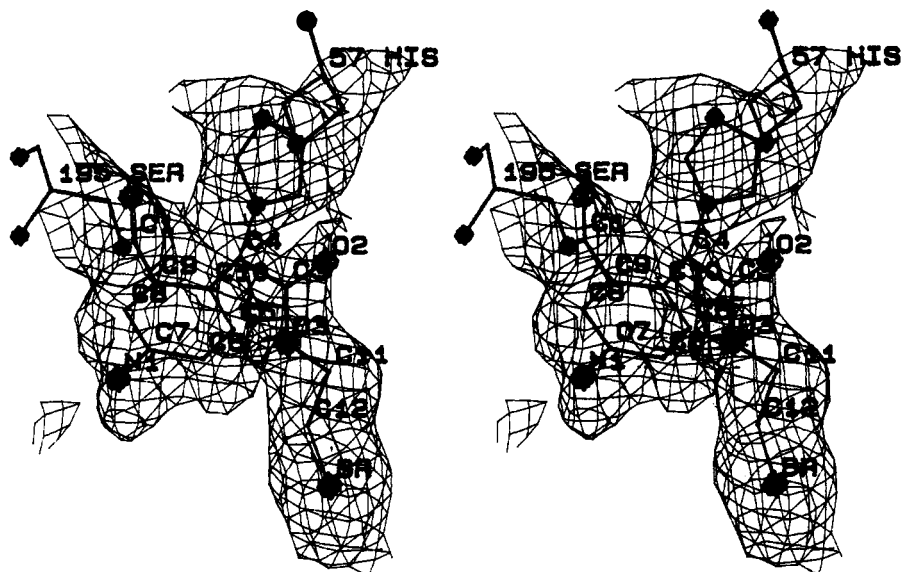


FIGURE 2: Stereoview of the final electron density difference ("omit") map of the active site region of porcine pancreatic elastase complexed with 7-amino-3-(2-bromoethoxy)-4-chloroisocoumarin. The inhibitor, Ser 195, and His 57 were removed from the protein model used for phasing, thus showing continuous densities at the two positions where the inhibitor is bound to the enzyme. The contour level is 1.6σ , and the σ value is $0.07 e/\text{\AA}^3$.

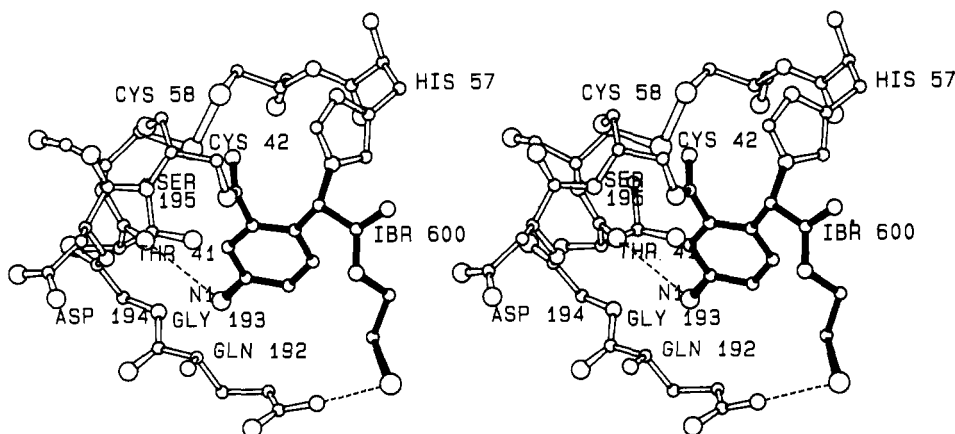


FIGURE 3: Stereoview of hydrogen bonding in the active site of the title complex (drawn by using the program BALLSTICK by R. Radhakrishnan, unpublished results). The inhibitor is drawn in heavy lines.

link from the C4 atom to the His 57 N ϵ 2 atom. The final refined model of the active site, including hydrogen bonding, is given in Figure 3.

While stereochemical (*R* or *S*) assignment of the C4 atom cannot be made unambiguously, the *S* configuration fits the electron density better and was taken as the correct structure. The bromoethoxy side chain of the inhibitor is directed toward the S₃ pocket, enclosed by residues Gln 192, Val 216, and Ser 217. The amino group of the inhibitor is directed toward the S₂' subsite [subsite nomenclature of Schechter and Berger (1987)] comprised of residues His 40, Thr 41, Leu 143, Leu 151, Gln 192, and Gly 193.

In addition to two covalent linkages between the enzyme and the inhibitor, the complex is further stabilized by hydrogen bonding (Figure 3) and various van der Waals interactions. Because of the proximity of the bromoethoxy side chain to Gln 192, the Br atom makes a weak hydrogen bond (3.2 Å) with Gln 192 N ϵ 2. The amino nitrogen atom at the 7-position points toward the S₂' subsite and makes a H bond (3.06 Å) to the carbonyl oxygen atom of Thr 41.

van der Waals contacts in previously determined PPE–isocoumarin complexes (Meyer et al., 1985; Powers et al., 1990) forced the imidazole ring of His 57 into the "out" conformation. Here the "in" conformation corresponds to a

covalent linkage (His 57 N ϵ 2–C4). The distance of Ser 195 O γ from His 57 N ϵ 2 is 3.85 Å vs 3.2 Å found between these two atoms in the native structure (Meyer et al., 1988). The His 57 imidazole ring is tilted approximately 30° away from Asp 102 with respect to the ring orientation in the native structure, due to inhibitor binding. This causes an unfavorable angle for hydrogen bonding between Asp 102 O δ 1 and His 57 N δ 1 although the distance between them is 3.05 Å (the donor H...acceptor angle is 110°; the H atom bonded to His 57 N δ 1 points away from the lone pair electrons of Asp 102 O δ 1). The dual attachment of inhibitor to enzyme causes a rather tight fit to occur between participating groups and atoms.

The rms deviation between the native and the title structure for 801 backbone (NCCO) atoms is 0.22 (0.09) Å when compared to the earlier solved 7-amino-4-chloro-3-methoxyisocoumarin complex with PPE, for 796 common backbone atoms the rms agreement is 0.22 (0.09) Å, and with 4-chloro-3-ethoxy-7-guanidinoisocoumarin–PPE complex, for 754 common backbone atoms, the rms agreement is 0.175 (0.07) Å. This further confirms that the simple serine proteases are "lock and key" enzymes (Fisher, 1894) in contrast to thrombin, which exhibits greater flexibility of the 60 and 148 "lip" (insertion) regions upon binding to substrates (Bode

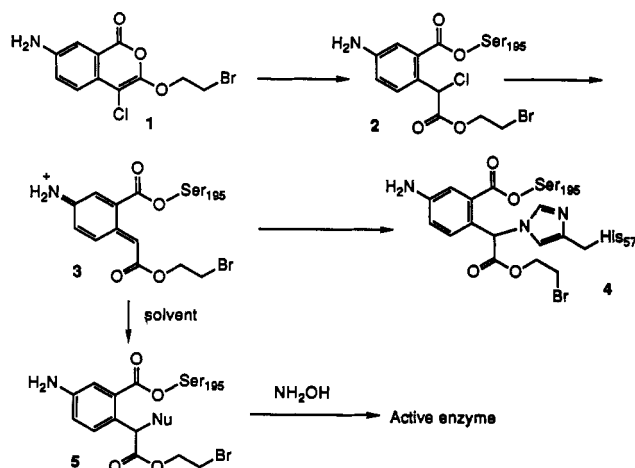


FIGURE 4: Proposed mechanism of inhibition of PPE by 7-amino-3-(2-bromoethoxy)-4-chloroisocoumarin.

et al., 1989). Even the necessary distortions required for dual covalent attachment require only slight distortion of backbone atoms.

Inhibition Kinetics. Several additional 7-substituted 3-(bromoalkoxy)-4-chloroisocoumarins were synthesized, and the rates of inhibition of PPE by these compounds are shown in Table IV. Generally, the 3-(bromoethoxy) compounds were more potent inhibitors toward PPE than 3-(bromopropoxy)-isocoumarin by 2 orders of magnitude in their second-order inhibition constants ($k_{\text{obs}}/[\text{I}]$). The 7-[(phenylacetyl)amino] and several bulky alkylureido or (arylalkyl)ureido derivatives of the bromoethoxy compound were 3–10-fold more potent inhibitors of PPE than the corresponding 7-amino compound. Surprisingly, 3-(2-bromoethoxy)-4-chloro-7-[(phenyl-carbamoyl)amino]isocoumarin is a poor inhibitor of PPE and has less inhibitory potency than the amino compound (Table IV). The second-order inactivation rate constant for reaction of PPE with most of the 7-(alkylureido)- or 7-(arylalkyl)-ureido]isocoumarins were biphasic with an initial rapid inhibition (60–80% inactivation) for the first 1–2 min, followed by a slower rate for the remainder of the reaction.

Deacylation Kinetics. The solution stability of PPE inactivated by 7-amino-3-(2-bromoethoxy)-4-chloroisocoumarin at pH 7.5 was tested. Excess inhibitor in the inactivated PPE mixture was removed by centrifugation twice at 0 °C for 1 h by using an Amicon microconcentrator 10. No enzymatic activity was found in the PPE–inhibitor mixture after standing at room temperature for a few days. The reactivation of inhibited PPE was also performed by the addition of 0.38 M NH_2OH ; 30% of the enzymatic activity was regained after a few hours, and no further activity was regained even after a few days.

DISCUSSION

Crystallographic Evidence of the Proposed Reaction Mechanism. 3-Alkoxy-7-amino-4-chloroisocoumarins are potent inhibitors of PPE (Harper & Powers, 1985; Powers et al., 1990). Both 7-amino and 4-chloro moieties are now known to be required for the formation of a stable acylated enzyme–inhibitor complex. The 3-alkoxy group is believed to be situated in the S_1 pocket in the initial PPE–inhibitor complex. The mechanism for the inhibition of serine proteases by these compounds was postulated on the basis of the kinetic results (Harper & Powers, 1985) and is shown in Figure 4 for 7-amino-3-(2-bromoethoxy)-4-chloroisocoumarin (1). The acyl enzyme (2) would initially be formed by the attack of Ser 195, followed by the postulated formation of a quinone imine

methide intermediate (3). This intermediate could be attacked either by His 57 to form a covalent linkage (4) or by a solvent molecule [e.g., 4-acetoxy in the complex of PPE with 7-amino-4-chloro-3-methoxyisocoumarin (Meyer et al., 1985)] to form another acyl enzyme (5), which could be reactivated by NH_2OH .

Although X-ray structure analysis shows that the double covalent linkage was found in the PPE–inhibitor complex under the conditions of cocrystallization and data collection, the reactivation experiment indicated 30% of E–I complex can be reactivated by NH_2OH at pH 7.5, suggesting that 70% of the enzyme was doubly linked and 30% of the enzyme singly linked to the inhibitor under conditions of the reaction. Residual electron density did not give evidence for a detectable population (roughly >10% occupancy) of an alternative binding mode for the cocrystallization conditions. The analysis of an isocoumarin + trypsin complex (Chow et al., 1990), which proceeded approximately in parallel to this study, exhibits such a dual occupancy, giving us a realistic basis for comparison. Both 7-amino-4-chloro-3-methoxyisocoumarin and 7-amino-4-chloro-3-ethoxyisocoumarin also regained 30–40% of activity after addition of NH_2OH (Harper & Powers, 1985).

Since the X-ray studies did not indicate the presence of the chloroacyl enzyme (2) and therefore we lack evidence on its chirality, we could presume the *S* chirality on the basis of the earlier PPE complex with 4-chloro-3-ethoxy-7-guanidinoisocoumarin which resulted only in the acyl enzyme. The doubly covalent adduct in the title complex also has the *S* configuration, suggesting the retention of chirality in the reaction leading to the final irreversible binding from the acyl enzyme complex. These results are consistent with a postulated mechanism involving the formation of the quinone imine methide intermediate (3). The direct $\text{S}_{\text{N}}2$ nucleophilic displacement of the Cl atom by His 57 would involve an inversion of chirality, and this mechanism is thereby ruled out.

The formation of the quinone imine methide intermediate and the nucleophilic attack by His 57 presume a neutral (His 57) imidazole ring. However, crystal growth and data collection occurred at pH 5.0, well below the presumed pK_a (6.0) of His. The pK_a of His 57 in the native or “in” position, as part of the catalytic tetrad, is a matter of conjecture. Upon binding with the inhibitor in the neutral or acidic region, the protonation equilibrium of His 57 may shift toward the deprotonated state. This may lead to overall proton release from the system (Nakatani et al., 1975) and may favor alkylation by His 57. While simultaneous attack of both Ser 195 and His 57 cannot be ruled out, the steps leading to and resulting from ring cleavage, especially the conformational rearrangements of ring substituents, cause us to prefer a dynamic, sequential series of events.

Among the 3-alkoxy-7-amino-4-chloroisocoumarins, the compounds with 3-methoxy, 3-ethoxy, or 3-(2-bromoethoxy) substituents are better inhibitors of PPE (with $k_{\text{obs}}/[\text{I}]$ values of 710–1040 $\text{M}^{-1} \text{s}^{-1}$) than the 3-propoxy compound (Powers et al., 1990). The decrease in the inhibition rates as the size of the 3-alkoxy group is increased is consistent with the fact that PPE prefers a small hydrophobic residue in the S_1 pocket. The 7-amino-3-(2-bromoethoxy)-4-chloroisocoumarin inhibited PPE with a $k_{\text{obs}}/[\text{I}]$ value of 1000 $\text{M}^{-1} \text{s}^{-1}$ and was more reactive than expected. It was presumed that the interaction of the Br atom with an amide N atom forming a hydrogen bond had occurred at the active site.

The original purpose of the design of this inhibitor with the 3-(bromoethoxy) side chain was to mimic the CCSC side chain

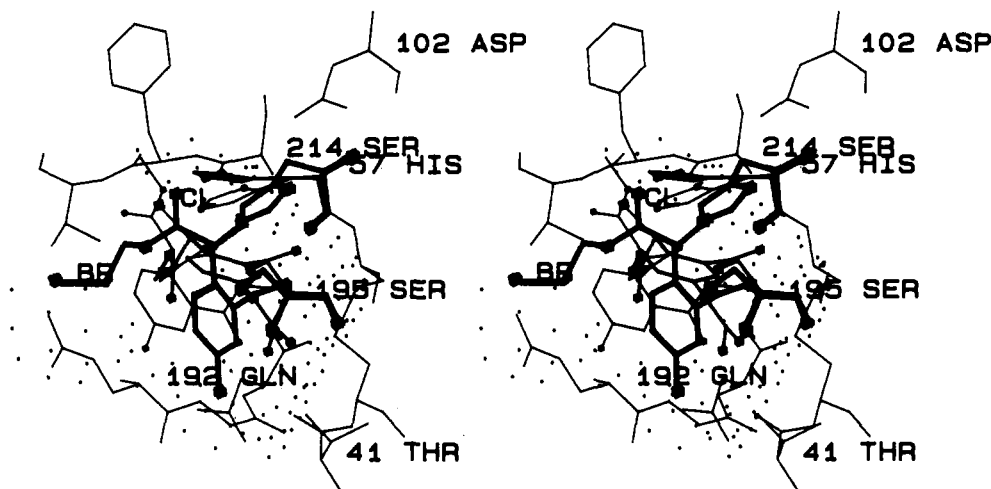


FIGURE 5: Stereoview of 7-amino-4-chloro-3-methoxyisocoumarin (Meyer et al., 1985), 4-chloro-3-ethoxy-7-guanidinoisocoumarin (Powers et al., 1990), and the present inhibitor in the active site of PPE. The figure was obtained with FRODO with the BLOB (BLOB option introduced by Andreas Karrer, unpublished work) radius for the present inhibitor set at 0.25 Å (heavy lines), for the 7-guanidinoisocoumarin structure of 0.17 Å (medium lines, Cl labeled in the S_1 pocket), and for 7-amino-3-methoxy-4-chloroisocoumarin at 0.1 Å (thin lines, phenyl ring to the left). The van der Waals contact surface of the title complex is depicted as a dotted surface defined as a double van der Waals surface less than twice the van der Waals radii of active site atoms (FRODO function INTER).

of Met 358 in the α 1-protease inhibitor, which fits tightly the S_1 subsite in serine proteases and thus is important for the binding and inhibition of HLE by α 1-protease inhibitor (Johnson & Travis, 1978). This inhibitor with a linear 3-(bromoethoxy) side chain was therefore expected to bind similarly, with the linear chain occupying the primary specificity pocket, S_1 , in a manner similar to that observed in previous studies (Johnson & Travis, 1978; Meyer et al., 1985; Powers et al., 1990). Surprisingly, the present X-ray structure analysis resulted in a completely different positioning of this bromoethoxy chain, namely, in the S_3 subsite of the active site (favoring a hydrogen bond between the negatively charged bromine atom and Gln 192 $N\epsilon 2$ in the active site). Besides revealing important new interactions of the inhibitor with the active site of PPE, these results show the limitations of our understanding of the enzyme–inhibitor binding modes and the limited predictive ability of molecular modeling.

Comparison of Different Inhibitor Binding Modes in PPE–Isocoumarin Complexes. Of the three heterocyclic isocoumarin inhibitors bound to PPE thus far studied crystallographically by our group, this complex was the first to exhibit a doubly covalent linkage with PPE. Figure 5 is a superimposed display of the three isocoumarin inhibitors (Meyer et al., 1985; Powers et al., 1990) in the active site region. The important differences found between these structures include the presence of the intact Cl atom in the case of 4-chloro-3-ethoxy-7-guanidinoisocoumarin structure and the solvent-derived acetoxy group in the S_1 pocket replacing the Cl atom in the structure of 7-amino-4-chloro-3-methoxyisocoumarin, and the absence of the Cl atom with formation of a covalent link from His 57 $N\epsilon 2$ to C4 of the inhibitor in the title structure. Whereas in the 7-amino-4-chloro-3-methoxyisocoumarin complex the benzoyl carbonyl oxygen atom is partially in the oxyanion hole formed between amide ($>NH$) groups of Gly 193 and Ser 195, this oxygen atom is entirely out of the oxyanion hole in the other two complexes (this would be expected to retard deacylation). In both the earlier complexes the methoxy and ethoxy side chains are situated in the S_1 subsite comprised of Cys 191, Gln 192, Gly 193, Ser 195, Thr 213, Ser 214, Phe 215, Val 216, Thr 226, and Val 227. In the present complex, we find the bromoethoxy side chain to be displaced toward the S_3 pocket formed by Gln 192, Val 216, and Ser 217, with the Br atom forming a weak hydrogen bond

(3.2 Å) with Gln 192 $N\epsilon 2$. In the 7-guanidinoisocoumarin complex, the aromatic ring is situated in such a way that the guanidino group is within H-bonding distance to the Thr 41 carbonyl O and $O\gamma$ atoms. In the title complex, the ring is positioned so that the amino N atom is pointed toward the S_2' subsite and makes a hydrogen bond (3.2 Å) with Thr 41 O. In the 7-amino-4-chloro-3-methoxyisocoumarin + PPE complex the aromatic ring is displaced and the amino N atom is 6.35 Å from Thr 41. In the present structure, the His 57 imidazole ring is found in the “in” position similar to the native structure ($\Delta X_2 = 30^\circ$). In the other two structures, the imidazole ring is rotated away from the “in” position; the shift is greater for 7-guanidinoisocoumarin ($\Delta X_1 = 109^\circ$ and $\Delta X_2 = 86^\circ$) than that found for the 7-amino-4-chloro-3-methoxyisocoumarin ($\Delta X_1 = 86^\circ$ and $\Delta X_2 = 59^\circ$). In the title complex the electronegative Br atom is attracted by the $N\epsilon 2$ of Gln 192 and may stabilize the orientation of the bromoethoxy side chain toward the S_3 subsite. Figure 5 also shows the inhibitor–enzyme van der Waals surface intersection for the title complex.

Comparison of the Doubly Covalent Bound Isocoumarin Complexes with PPE and Trypsin. Shortly after this structure analysis, we independently captured a doubly linked isocoumarin inhibitor bound to trypsin. This inhibitor [4-chloro-3-ethoxy-7-guanidinoisocoumarin complex (Chow et al., 1990)] showed two simultaneous (statistically averaged) binding modes, the first an acyl enzyme complex without a covalent link with His 57 and the second one a doubly covalent linked structure similar to the present complex. Figure 6 compares the binding of the two doubly covalent bound isocoumarin structures. The model of 4-chloro-3-ethoxy-7-guanidinoisocoumarin in the trypsin complex with the single covalent link with Ser 195 $O\gamma$ is also shown in Figure 6. Since Val 216 and Thr 226 residues in elastase replace the corresponding Gly residues in trypsin and chymotrypsin in the binding pocket, the binding of 3-alkoxyisocoumarins in PPE is quite different from that seen in trypsin. In the various binding modes of isocoumarins to PPE, the amino group or the guanidinium group at the 7-position of the aromatic ring points toward the S_2' subsite of PPE, whereas in trypsin, the S_1 pocket has a negatively charged Asp 189 and binds to the charged guanidinium group, with a water molecule facilitating the hydrogen bond between both the charged groups. Thus

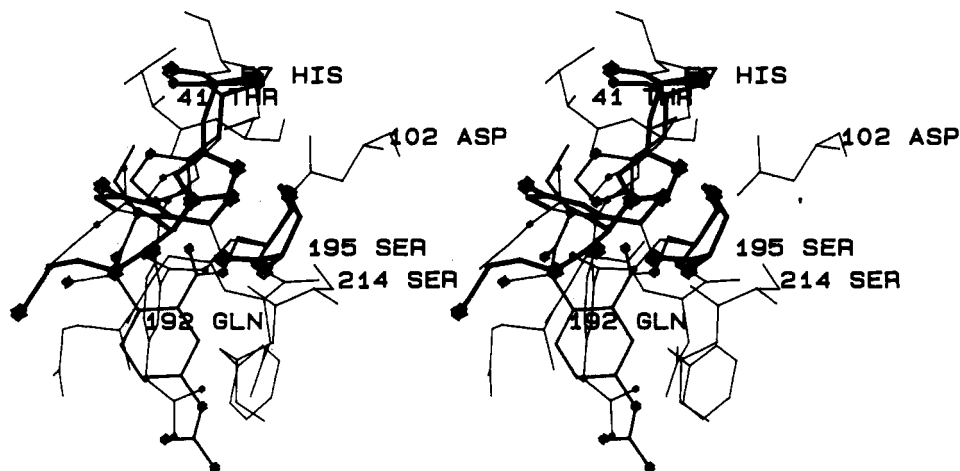


FIGURE 6: Stereo superposition and comparison of the binding of two isocoumarin structures having covalent bonds to His 57, one with PPE (title complex) and the other with trypsin (4-chloro-3-ethoxy-7-guanidinoisocoumarin with trypsin; Chow et al., 1990). BLOB (hetero atoms, N, O, Br) radii of 0.25 Å are used for the title complex (heavy lines); the 7-guanidinoisocoumarin complex with trypsin shows two binding modes, one singly bound to Ser 195 (shown with BLOB radius = 0.17 Å, medium lines) and another doubly bound to Ser 195 and His 57 (shown with BLOB radius = 0.1 Å, thin lines). The corresponding His 57 and Ser 195 amino acids are represented by thick, medium, and thin lines, respectively.

the aromatic ring of the inhibitor is flipped by 180° from the S_1 to S_2' subsite in the case of elastase and trypsin.

The chirality of the covalent adduct formed with His 57 is *S* in the title complex while it is *R* in both doubly covalent and the chloracyl derivatives of trypsin. The positions of benzoyl carbonyl oxygen atoms in both complexes are also quite different. In the trypsin complex, it is partly in the oxyanion hole, forming an H bond with the amide nitrogen atom of Gly 193, while in the PPE complex it is far removed [ca. 3.7 Å from the amide (>NH) group of Ser 195 and 5.5 Å from that of Gly 193] from the oxyanion hole.

Summary of the Earlier Inhibitors to Serine Proteases Forming a Double Covalent Link. A β -lactam inhibitor forming a doubly covalent linkage to PPE is the first instance of such irreversible binding to PPE (Navia et al., 1987). In that complex, the β -lactam ring has reacted with Ser 195, and His 57 has reacted with expulsion of a leaving group at the cephalosporin 3'-position to form two covalent bonds with the active site of PPE. The covalent bond to N ϵ 2 of His 57 is formed with the rotation of His 57, and its N δ 1 atom is within hydrogen-bonding distance from Asp 60 O δ 2, a distance comparable to the observed interaction of His 57 N δ 1 with Asp 102 O δ 1 in the catalytic triad.

Chloromethyl ketones are another class of inhibitors whose mechanism involves reaction with a nucleophilic histidine. In the crystal structure of the HLE complex with a valine chloromethyl ketone (Wei et al., 1988), there are covalent bonds from the valine chloromethyl ketone moiety of the inhibitor to His 57 N ϵ 2 and Ser 195 O γ of the enzyme. In the HLE complex with an alanine chloromethyl ketone (Navia et al., 1989), the terminal carbon atom of the alanine chloromethyl ketone moiety is bonded covalently to His 57 N ϵ 2 and the ketone carbon atom of the Ala residue reacts with Ser 195 to form a tetrahedral ketal.

In the PPE complex with (carbobenzyloxy)alanyl-leucine-boronic acid (Takahashi et al., 1989), we find His 57 N ϵ 2 is involved in a coordinate covalent bond with the boron atom. The mode of inhibition is believed to be due to formation of a hemiacetal-like intermediate with the catalytic serine O γ atom of the enzyme, resembling the tetrahedral intermediate postulated on the pathway for substrate hydrolysis.

Inhibition Kinetics. The relative reactivities of 7-substituted derivatives of 3-(2-bromoalkoxy)-4-chloroisocoumarins can

now be explained on the basis of the crystal structure. The 7-substituted 4-chloro-3-(2-bromoethoxy)isocoumarins are more potent inhibitors than the corresponding 3-bromopropoxy derivatives. The poor inhibition of the latter compounds are due to the bulky size of the bromopropoxy group, which cannot fit into the S_3 pocket. The hydrogen bonding between the Br atom and Gln N ϵ 2 which exists weakly in the 7-amino-3-(2-bromoethoxy)-4-chloroisocoumarin structure would also be interrupted in the 3-bromopropoxy compounds. Several bulky *N*-alkylureido and *N*-(arylalkyl)ureido derivatives [*tert*-butyl-, isopropyl-, or (methylbenzyl)ureido] are better inhibitors of PPE than the parent amino compound, since the *N*-alkyl substituent could make a favorable interaction with the nearby S_2' or S_3' hydrophobic subsites. In the S_2' region, Leu 151 is at ca. 6.7 Å from the 7-amino group of the isocoumarin inhibitor and Leu 143 is at ca. 8 Å from the 7-amino group. In the S_3' region, Leu 63 is at ca. 9.4 Å from the amino group and Tyr 35 is at ca. 8 Å from the amino group. The low inhibition rate constant of 3-(2-bromoethoxy)-4-chloro-7-[(phenylcarbamoyl)amino]isocoumarin toward PPE was surprising, since the corresponding 3-methoxy- and 3-ethoxyisocoumarins were better inhibitors than the parent 7-amino compounds (Powers et al., 1990). However, the 7-[(phenylacetyl)amino] compound, which has a similar sized substituent as the phenylureido compound, was a potent PPE inhibitor. We believe the inhibitory potency of the 7-(phenylureido) derivative is due to the rigidity of the phenylureido group, which results in some interference with other residues on the enzyme. The inhibition rates of PPE by 7-(alkylureido)isocoumarins were biphasic, which has also been observed in the case of 7-(alkylureido)-4-chloro-3-ethoxyisocoumarins (Powers et al., 1990). This can be explained by the existence of a different ratio of trans or cis isomers around the ureido group in the inhibitor which react with PPE with different rates.

SUMMARY AND CONCLUSION

We have shown that PPE in its native state or bound to a variety of inhibitors retains its tertiary structure and thus can be called a "lock and key" enzyme (Fisher, 1894). While the "lock and key" concept holds thus far for the "lock" part of serine proteases, the "keys" exhibit such a variety of binding modes as to challenge the chemist and crystallographer to learn the rules that govern these reactions. The title complex is the first PPE-isocoumarin complex to exhibit an irreversible

binding to His 57 in this class of substituted 7-amino-4-chloroisocoumarins. The reactions leading to the covalent attachment of His 57 to the inhibitor indicate that it is a mechanism-based inhibitor. This is the second heterocyclic irreversible inhibitor of porcine pancreatic elastase with two covalent links to the enzyme, the first one being a β -lactam inhibitor (Navia et al., 1987). It is also the fifth heterocyclic inhibitor (cf. Table II) and the third isocoumarin inhibitor of PPE to be studied crystallographically. Our earlier studies of three complexes of PPE with heterocyclic inhibitors including the two PPE–isocoumarin complexes with different substituents at the 3- and 7-positions show that *the binding geometries are all distinctly different*. The title complex with an irreversible reaction complicates the story further by exhibiting a binding geometry distinctly different from the other two isocoumarin structures thus far studied. Why was such a geometry not observed before? Or, more puzzling, why is it observed to occur at roughly at 50% occupancy in the related (Chow et al., 1990) trypsin + 4-chloro-3-ethoxy-7-guanidinoisocoumarin complex? We are forced to conclude that our understanding of forces contributing to the binding of small molecules to enzymes is incomplete and that additional, high-resolution crystallographic studies will be required. The binding mode of long (>4 amino acids) peptide substrates and inhibitors to the serine proteases is well established and thus may be used with some confidence as a template for computer modeling of homologous complexes with homologous members of the serine proteases family. However, the desire to develop potent and specific heterocyclic inhibitors for serine proteases continues to be frustrated by this noncanonical binding. Eventually, molecular dynamics calculations may be able to predict preferred binding loci, but at present, high-resolution structure analysis is of overwhelming importance in probing the binding and reaction geometries of heterocyclic inhibitors. Structure analysis of additional elastase–inhibitor complexes can hopefully pave the way for designing an effective therapy for pulmonary emphysema and other degenerative diseases.

ACKNOWLEDGMENTS

We thank Prof. George Phillips for use of the Optronics film scanner.

Registry No. L-Ser, 56-45-1; L-His, 71-00-1; L-Gln, 56-85-9; L-Thr, 72-19-5; 7-amino-3-(3-bromopropoxy)-4-chloroisocoumarin, 113251-20-0; 7-amino-3-(2-bromoethoxy)-4-chloroisocoumarin, 126062-22-4; 3-(2-bromoethoxy)-7-[(*tert*-butylcarbamoyl)amino]-4-chloroisocoumarin, 131068-60-5; 3-(2-bromoethoxy)-4-chloro-7-[(isopropylcarbamoyl)amino]isocoumarin, 131068-61-6; 3-(2-bromoethoxy)-4-chloro-7-[(phenylcarbamoyl)amino]isocoumarin, 131068-62-7; 7-[(benzylcarbamoyl)amino]-3-(2-bromoethoxy)-4-chloroisocoumarin, 131068-63-8; 3-(2-bromoethoxy)-4-chloro-7-[[[(*R*)-methylbenzyl]carbamoyl]amino]isocoumarin, 131068-64-9; 3-(2-bromoethoxy)-4-chloro-7-[[[(*S*)-methylbenzyl]carbamoyl]amino]isocoumarin, 131068-65-0; 3-(2-bromoethoxy)-4-chloro-7-[(phenylacetyl)amino]isocoumarin, 131068-66-1; 3-(3-bromopropoxy)-4-chloro-7-[(phenylcarbamoyl)amino]isocoumarin, 131068-67-2; 7-[(benzylcarbamoyl)amino]-3-(bromopropoxy)-4-chloroisocoumarin, 131068-68-3; 3-(3-bromopropoxy)-4-chloro-7-[(phenylacetyl)amino]isocoumarin, 131068-69-4; elastase, 9004-06-2.

REFERENCES

Bode, W., Mayr, I., Baumann, U., Huber, R., Stone, S. R., & Hofsteenge, J. (1989) *EMBO J.* 8, 3467–3475.
Burchardi, H., Stokke, T. & Hensel, T., Koestering, H.,

Ruhlof, G., Schlag, G., Heine, H., & Hori, W. H. (1984) *Adv. Exp. Med. Biol.* 167, 319–333.
Chow, M. M., Meyer, E. F., Jr., Bode, W. Kam, C. M., Radhakrishnan, R., Vijayalakshmi, J., & Powers, J. C. (1990) *J. Am. Chem. Soc.* (in press).
Fisher, E. (1894) *Ber. Deutsch. Chem. Ges.* 27, 2985–2993.
Geokas, M. C., Rinderknecht, H., Swanson, V., & Haverback, B. J. (1968) *Lab. Invest.* 19, 235–239.
Harper, J. W., & Powers, J. C. (1985) *Biochemistry* 24, 7200–7213.
Janoff, A. (1973) in *Molecular Basis of Biological Degradative Processes* (Berlin, R. D., Herrman, H., Lepow, I. H., & Tanzer, J. M., Eds.) pp 225–260, Academic Press, New York.
Janoff, A. (1978) in *Neutral Proteases in Human Polymorphonuclear Leukocytes* (Havemann, K., & Janoff, A., Eds.) pp 390–417, Urban and Schwartzberg, Baltimore.
Johnson, D., & Travis, J. (1978) *J. Biol. Chem.* 253, 7142–7144.
Jones, T. A. (1978) *J. Appl. Crystallogr.* 11, 268–272.
Kennard, O. W., Watson, D. G., Allen, F. H., Isaacs, N. W., Motherwell, W. D. S., Peterson, R. C., & Town, W. G., Eds. (1972) *Molecular Structures and Dimensions*, Vol. A1, N. V. A. Oosthoek's Uitgevers Mij, Utrecht.
Lee, J. D., & Pakes, H. W. (1969) *Acta Crystallogr.* A25, 712–713.
Lungarella, G., Gardi, C., Desanti, M. M., & Luzi, P. (1985) *Exp. Mol. Pathol.* 42, 44–59.
Luzatti, V. (1952) *Acta Crystallogr.* 5, 802–810.
Messerschmidt, A., & Pflugrath, J. W. (1987) *J. Appl. Crystallogr.* 30, 306–315.
Meyer, E. F., Jr., Presta, L. G., & Radhakrishnan, R. (1985) *J. Am. Chem. Soc.* 107, 4091–4093.
Meyer, E. F., Jr., Cole, G., Radhakrishnan, R., & Epp, O. (1988) *Acta Crystallogr.* B34, 26–38.
Nakatani, H., Uehara, Y., & Hiromi, K. (1975) *J. Biochem.* 78, 611–616.
Navia, M. A., Springer, J. P., Lin, T. Y., Williams, H. R., Firestone, R. A., Pisano, J. M., Doherty, J. B., Finke, P. E., & Hoogsteen, K. (1987) *Nature* 327, 79–82.
Navia, M. A., McKeever, B. M., Springer, J. P., Lin, T. Y., Williams, H. R., Fluder, E. M., Dorn, C. P., & Hoogsteen, K. (1989) *Proc. Natl. Acad. Sci. U.S.A.* 86, 7–11.
Powers, J. C. (1976) *Trends Biochem. Sci.* 1 (9), 211–214.
Powers, J. C., Oleksyszyn, J., Lakshmi Narasimhan, S., Kam, C. M., Radhakrishnan, R., & Meyer, E. F., Jr. (1990) *Biochemistry* 29, 3108–3118.
Radhakrishnan, R., Presta, L. G., Meyer, E. F., Jr., & Wildonger, R. (1987) *J. Mol. Biol.* 198, 417–424.
Schechter, I., & Berger, A. (1967) *Biochem. Biophys. Res. Commun.* 27, 157–162.
Schwager, P., Bartles, K., & Jones, A. (1975) *J. Appl. Crystallogr.* 8, 275–280.
Schweizer, W. B., & Dunitz, J. D. (1982) *Helv. Chim. Acta* 65, 1547–1554.
Swanson, S. M. (1988) *Acta Crystallogr.* A44, 437–442.
Takahashi, L. H., Radhakrishnan, R., Rosenfield, R. E., Jr., & Meyer, E. M., Jr. (1989) *Biochemistry* 28, 7610–7617.
Tronrud, D. E., Ten Eyck, L. F., & Matthews, B. W. (1987) *Acta Crystallogr.* A43, 489–501.
Wei, A. Z., Mayr, I., & Bode, W. (1988) *FEBS Lett.* 234, 367–373.